J. Am. Ceram. Soc., 98 [3] 965–971 (2015)
DOI: 10.1111/jace.13391

journal

Local Fracture Toughness of Si_3N_4 Ceramics Measured using Single-Edge Notched Microcantilever Beam Specimens

Junichi Tatami,[‡,†] Masaki Katayama,[‡] Masahiro Ohnishi,[‡] Tsukaho Yahagi,[§] Takuma Takahashi,[§] Takahiro Horiuchi,[¶] Masahiro Yokouchi,[¶] Kouichi Yasuda,[‖] Do Kyung Kim,[††] Toru Wakihara,[‡] and Katsutoshi Komeya[‡]

[‡]Yokohama National University, Yokohama 240-8501, Japan

[§]Kanagawa Academy of Science and Technology, Kawasaki 213-0012, Japan

[¶]Kanagawa Industrial Technology Center, Ebina 243-0735, Japan

[‖]Tokyo Institute of Technology, Tokyo 152-8552, Japan

[††]Korea Advanced Institute of Science and Technology, Daejeon 305-701, Korea

Local fracture toughness gives us useful and important information to understand and improve mechanical properties of bulk ceramics. In this study, the local fracture toughness of silicon nitride (Si_3N_4) ceramics was directly measured using single-edge notched microcantilever beam specimens prepared by the focused ion beam technique. The measured fracture toughness of grain boundary of the Si_3N_4 ceramics is higher than the fracture toughness of SiAlON glass, which exists in the grain boundaries of Si_3N_4 ceramics. It is also shown that the fracture toughness of grain boundary depends on the rare earth oxide added as a sintering aid, which is expected in terms of the difference in the grain-boundary structure. The fracture toughness of a single β-Si_3N_4 grains is higher than the grain-boundary fracture toughness. It was also higher than the value estimated from *ab initio* calculations and surface energy, which means that any dissipative energy should be included in the fracture toughness of a grain in spite of the brittle fracture in Si_3N_4. The fracture toughness of polycrystals of Si_3N_4 ceramics measured using single-edge notched microcantilever beam specimens is intermediate between those of grains and grain boundaries, and it agrees with the estimated initial value of the *R*curve, K_{I0}, in Si_3N_4 ceramics.

I. Introduction

Si_3N_4 ceramics are one of the most typically used engineering ceramics similar to Al_2O_3 and ZrO_2. They have been applied to bearing elements, substrates, and so on[1–3] because of their advantages such as high fracture toughness, high strength, and high corrosion and thermal resistance owing to their high covalent Si–N bonding and elongated β-Si_3N_4 grain structure. Si_3N_4 ceramics are usually densified by liquid phase sintering at high temperatures.[4,5] Elongated β-Si_3N_4 grains are developed during densification and the liquid remains as SiAlON glass in the grain boundaries after cooling.[6,7] As a result, cracks propagate to the grain boundary because they are more brittle and weaker than the elongated β-Si_3N_4 grains, and therefore, the microstructure of Si_3N_4 ceramics controls the mechanical properties.[8–10] Although the fracture toughness of grains and grain boundaries of Si_3N_4 ceramics is an important quantitative parameter for controlling the crack propagation behavior and mechanical properties of the bulk ceramics, it has not actually been measured yet. This shortcoming is not limited to only Si_3N_4 ceramics. There are hardly any studies on the grain-boundary fracture toughness of other ceramics as well.

In the previous studies, the fracture toughness of single crystals and bicrystals was estimated on the supposition that they regarded as a grain and grain boundary, respectively.[11–15] However, the grains and grain boundaries in the actual ceramics are not always the same as those in bulk single crystal and the bicrystal interface because the structure and properties in actual ceramics are affected by the process conditions. Furthermore, it is difficult to obtain bulk single crystals and bicrystals in most inorganic substances such as Si_3N_4. Attempts have been made to estimate the bonding strength and/or toughness of the grains and grain boundaries from the crack propagation behavior in previous studies.[16–18] However, these studies do not provide direct information of local mechanical properties.

The *R* curve is very important for understanding the high strength and toughness of Si_3N_4 ceramics. The increase in the *R* curve strongly depends not only on the grain size and shape but also on the additives.[19,20] The initial value of the *R* curve, K_{I0}, is especially important for understanding the fatigue properties of Si_3N_4 ceramics,[21,22] which include the effect of the crack propagation behavior and the fracture toughness of the grains and grain boundaries. In the previous studies, estimation of K_{I0} was limited to crack-opening displacement of Vickers indentation or by compliance technique.[23,24]

Focused ion beam (FIB) technique is the method to prepare very small specimens for TEM and so on. In some previous studies, FIB method also has been applied to make a specimen or a sharp notch for fracture toughness measurement.[25–27] However, there has been no reports to measure the fracture toughness of grain boundary, grain, and polycrystal of Si_3N_4 ceramics using a single-edge notched microcantilever beam specimens. In particular, the fracture toughness of polycrystal of Si_3N_4 ceramics should correspond to K_{I0}.

In this study, we show the local fracture toughness of the grains, grain boundaries, and polycrystals of Si_3N_4 ceramics using single-edge notched microcantilever beam specimens obtained by direct sampling from bulk Si_3N_4 ceramics through the FIB technique, followed by fracture tests using a nanoindentor. This technique is applicable to almost all

V. Sglavo—contributing editor

Manuscript No. 35351. Received July 25, 2014; approved November 21, 2014.
[†]Author to whom corrrespondence should be addressed. e-mail: tatami@ynu.ac.jp

materials, and we can measure not only the fracture toughness of the grains and grain boundaries but also the strength, fatigue, and so on. Furthermore, we can evaluate the mechanical properties of any region, such as the neck of grains in porous materials, irregular regions such as secondary phases, corroded and damaged areas, surfaces, thin and thick films, fibers, and particles and their interfaces, all of which are impossible to measure by conventional techniques.

II. Experimental Procedure

(1) Fabrication of Si_3N_4 Ceramics by Adding Various Kinds of Rare Earth Oxides

Si_3N_4 ceramics were prepared by adding rare earth oxides (Y_2O_3, Lu_2O_3, Lu_2O_3) and Al_2O_3. Si_3N_4 (SN-E-10; Ube Industries, Ltd., Tokyo, Japan), RE_2O_3 (Y_2O_3, La_2O_3, Lu_2O_3) (RU; Shin-Etsu Chemical Co., Ltd., Tokyo, Japan), and Al_2O_3 (AKP-30; Sumitomo Chemical Co., Ltd., Tokyo, Japan) powders were used as raw materials. The powders were weighed in a weight ratio of 92:5:3. The mixed powders, an organic binder [Paraffin (melting point: 46°C–48°C), Junsei Chemical Co., Ltd., Tokyo, Japan], a dispersant (Seruna E503; Chukyo Yushi Co., Ltd., Nagoya, Japan), and a lubricant [Bis(2-ethyhexyl) phthalate, Wako Pure Chemical Industries, Ltd., Osaka, Japan] were ball milled for 96 h in ethanol using SiAlON balls and a silicon nitride pot. After mixing, the powders were sieved using a #60 sieve made of nylon to obtain granules. The powder mixtures were compacted using a WC/Co die at a pressure of 50 MPa, followed by cold isostatic pressing at a pressure of 200 MPa. After dewaxing by heating at 500°C for 3 h in air, the Si_3N_4 ceramics used to measure the fracture toughness of the grains and grain boundaries were fabricated by firing at 1900°C for 2 h in 0.9 MPa N_2. The samples used to measure the fracture toughness of Si_3N_4 polycrystals, the *R* curve, and to observe the crack propagation *in situ* were prepared by firing at 1800°C for 2 h in 0.9 MPa N_2. After gas pressure sintering, hot isostatic pressing was carried out at 1700°C for 1 h in 100 MPa N_2. Dense sintered bodies having an elongated grain microstructure were obtained, as shown in Fig. 1.

(2) Determination of Local Fracture Toughness Using Single-Edge Notched Microcantilever Beam Specimens

The surfaces of the Si_3N_4 ceramics were mechanically polished and etched by CF_4 plasma. The single-edge microcantilever beam specimens were machined using the FIB technique (XVision 200TB; SII NanoTechnology Co., Ltd., Chiba, Japan). The microcantilever beam was prepared under an acceleration voltage of 30 kV and beam currents of 27, 6.5, and 1.3 nA. After machining, a sharp notch along the targeted region, that is, grain, grain boundary, or polycrystal normal to its longitudinal direction, was carefully machined under an acceleration voltage of 30 kV and a beam current of 80 pA. Figures 2(a) and (b) show the surfaces of the Si_3N_4 ceramics before and after machining, respectively. The target area used to measure the fracture toughness (the grain boundary in the case of Fig. 2) is located on the bottom of the microcantilever beam specimen. As shown in Figs. 2(c) and (d), the width, thickness, and length of the microcantilever specimens were 1.5–5 μm, 2–4 μm, and 15 μm, respectively. Their section profile was pentagonal. Schematic illustration of the orientation of the notch and the beam was shown in Fig. 2(e). A sharp notch of which radius was less than 15 nm was machined at the grain boundary, as shown in Fig. 2(f). Figures 3 show the specimens used to measure the fracture toughness of a grain and polycrystal, respectively. The longitudinal direction of the specimen for the fracture toughness of the grain matched the elongated direction of a β-Si_3N_4 grain. In the Si_3N_4 polycrystal specimen, several grains exist at the notch tip.

The fracture load of the notched specimens was measured using a nanoindentor (TI-950; Hysitron, Inc., Minneapolis, MN) by loading at a point 12 μm from the bottom of the cantilever beam. The loading point was previously decided upon by comparing the topographic image taken using atomic force microscopy equipped with the nanoindentor and the secondary scanning electron microscopy image observed before the fracture test. The load was applied to the specimens using a Bercovic-type diamond indenter under a loading rate of 30 μN/s.

To estimate the stress intensity factor, K_I, of the specimens, finite element method (FEM) analysis (ANSYS 13.0; ANSYS, Inc., Canonsburg, PA) was carried out using the geometry of the specimens and the critical load obtained by the fracture test. Wireframe and mesh images of the typical FEM model were shown in Fig. 4. In this study, elastic isotropy was assumed though Si_3N_4 has elastic anisotropy and intergranular glassy phase exists between Si_3N_4 grains. A notch in this model was regarded as a crack and very fine elements were located near the notch tip. K_I at the plain strain state was estimated from the crack-opening displacement, δ, at a distance from the notch tip, *r*, using the following equation[28]:

$$K_I = \sqrt{\frac{2\pi}{r}} \frac{E}{1-\nu^2} \frac{\delta}{8} \tag{1}$$

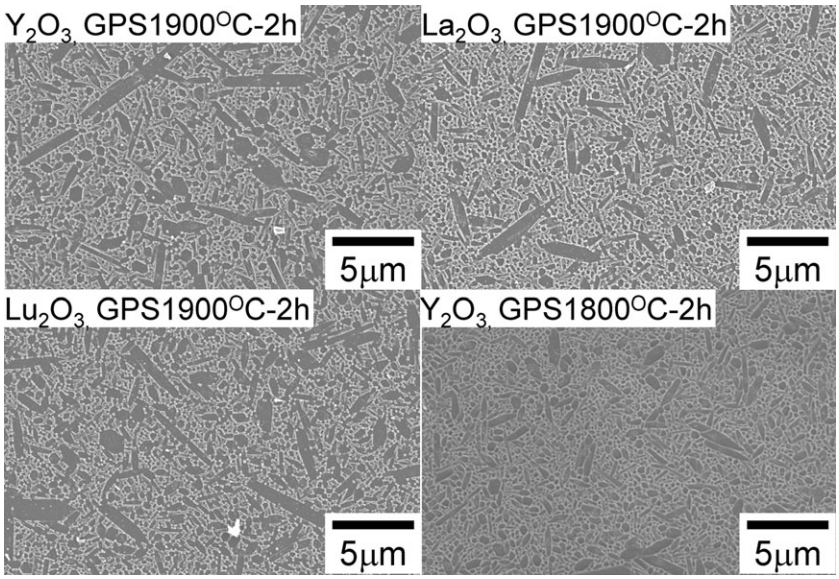

Fig. 1. SEM photographs of microstructures of the Si_3N_4 ceramics used in this study.

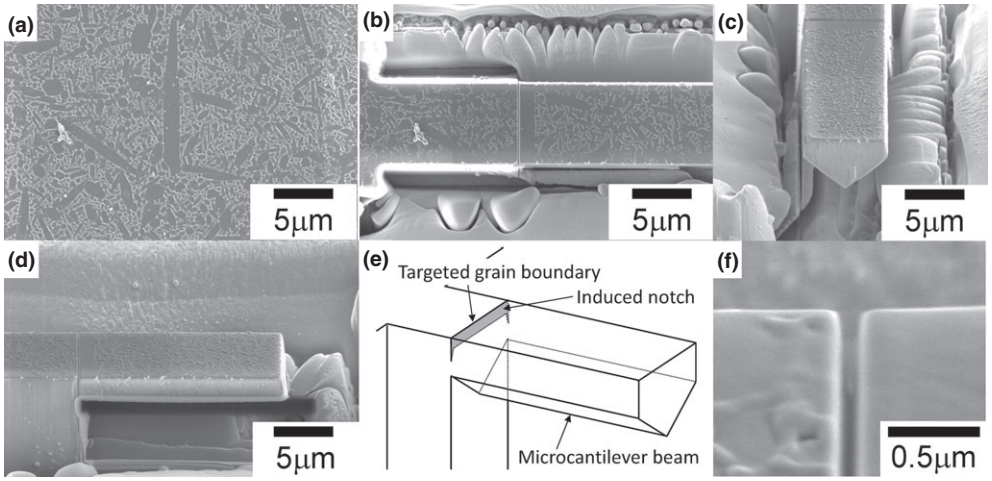

Fig. 2. Single-edge notched microcantilever beam specimen used to measure the fracture toughness of grain boundaries: (a) and (b) are the surface of Si_3N_4 ceramics before and after machining, respectively, and (c) and (d) are front and side views of the specimens, respectively. (e) Schematic illustration of the specimen. (f) The notch induced along the targeted grain boundary.

where E is the elastic modulus and ν is the Poisson ratio. 320 GPa and 0.25 as E and ν were used for the FEM analysis in this study, respectively. The value of K_I was plotted against the distance from the notch tip. A typical example of the relationship between K_I calculated from using the crack-opening displacement and the distance from the notch tip in the FEM analysis is shown in Fig. 4(d). K_I initially increased and then decreased with increasing distance from the crack tip. Since the value of the calculated K_I near the crack tip is inaccurate because of the singularity of the stress at the crack tip, the facture toughness was estimated by interpolating the value at a distance more than 25 nm from the notch tip, namely, at $r = 0$. Validation of the testing method was determined using single-crystal Si (see Appendix).

(3) In Situ Observation of Crack Propagation Behavior

In order to estimate the fracture behavior of Si_3N_4 ceramics, *in situ* observation of crack propagation was carried out using a very small testing machine equipped with a scanning probe microscope. The samples were cut to 4 mm × 1.5 mm × 20 mm and a half-chevron notch was machined at the center of the specimen to facilitate stable crack growth. The surfaces of the specimens were polished using a diamond slurry followed by plasma etching. The plasma etching was carried out in CF_4 gas for 2 s. The height of the remaining grain boundary was less than 2 nm. Crack propagation behavior was observed under loading in the dynamic force microcopy mode.

(4) Measurement of R Curve Over a Short Crack Length

The R curve over a short crack length was measured by surface cracks in flexure testing[29] to compare the fracture toughness measured using bulk specimens and with that of the microcantilever beam specimens. Si_3N_4 ceramics were cut into 3 mm × 4 mm × 30 mm samples and the surfaces were mechanically polished using a diamond slurry. A crack was induced using a Knoop indentor under loads of 19.6, 49, 98, and 196 N. The surface layer was removed to eliminate residual stress around the indentation and to control the size of the crack by grinding using a diamond slurry. The fracture stress was measured using a three-point bending test with a span of 30 mm and a crosshead speed of 0.5 mm/min. The fracture toughness was calculated using the following equations[30]:

$$K_{Ic} = Y \cdot \sigma_f \cdot \sqrt{a} \tag{2}$$

$$Y = \frac{\sqrt{\pi} \cdot M \cdot H_2}{\sqrt{Q}} \tag{3}$$

$$M = [1.13 - 0.09[a/c]] + \left[-0.54 + \frac{0.89}{[0.2 + [a/c]]} + 14[1 - a/c]^{24}\right] \cdot [a/W]^4 \tag{4}$$

$$H_2 = 1 - [1.22 + 0.12[a/c]] \cdot [a/W] + \left[0.55 - 1.05[a/c]^{0.75} + 0.47[a/c]^{1.5}\right] \cdot [a/W]^2 \tag{5}$$

$$Q = 1 + 1.464[a/c]^{1.65} \tag{6}$$

where a is the crack depth, $2c$ is the crack width, W is the specimen height, and σ_f is the fracture stress. The values of a and c were measured by SEM observation.

III. Results and Discussion

(1) Fracture Toughness of Grain Boundary of Si_3N_4 Ceramics

Figure 5 shows the facture surfaces of the specimens to evaluate the fracture toughness of grain boundary. In Fig. 5(a), it is observed that a crack propagated along the targeted grain boundary. On the other hand, the fracture surface is rough in the sample shown in Fig. 5(b), which means that a crack did not propagate along the targeted grain boundary. In this study, the fracture toughness of the grain boundary was calculated using only samples in which cracks propagated along the targeted grain boundary, as shown in Fig. 5(a).

Table I lists the fracture toughness values of grain boundaries of Si_3N_4 ceramics measured using single-edge notched microcantilever beam specimens. The fracture toughness of the grain boundaries varied from 1.5 to 2.3 MPa $m^{1/2}$. It is well-known that there is SiAlON glass containing rare earth ions, which were added as sintering aids, in the grain boundaries of Si_3N_4 ceramics.[6,7] The fracture toughness of the SiAlON glass has been reported to be less than

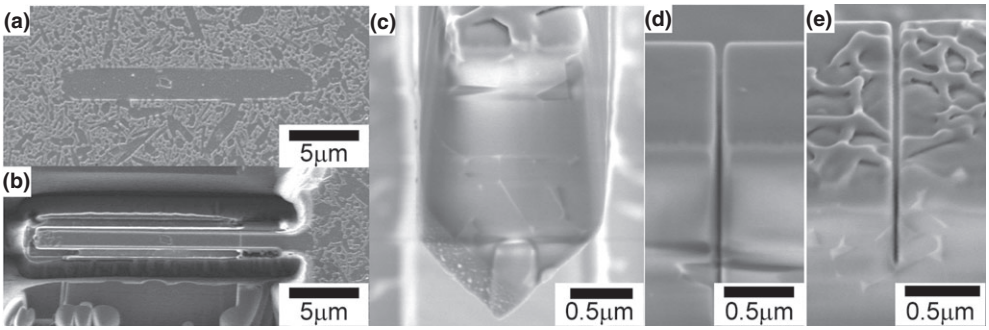

Fig. 3. Single-edge notched microcantilever beam specimen used to measure the fracture toughness of (a)–(d) a single Si_3N_4 grain and (e) polycrystal: (a) and (b) are the surface of Si_3N_4 ceramics before and after machining, respectively, and (c) is a front view of the specimen. (d) and (e) The notch induced in a Si_3N_4 grain and polycrystals, respectively.

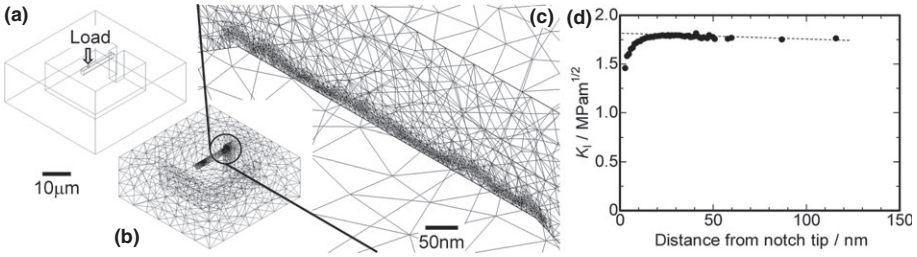

Fig. 4. (a) Wireframe and (b) mesh images for FEM analysis of single-edge notched microcantilever beam specimen. (c) is the enlarged view of the mesh image near the notch tip. (d) Relationship between the stress intensity factor and the distance from the notch tip estimated by FEM analysis. A dashed line indicates the regression line used to estimate K_I.

1 MPa $m^{1/2}$.[31,32] It was shown that the fracture toughness of the grain boundaries of Si_3N_4 ceramics measured in this study is higher than that of bulk SiAlON glass. This means that there is a possibility that the glassy phase in Si_3N_4 ceramics has a different amorphous structure from the bulk SiAlON glass.

The fracture toughness of the grain boundaries also depended on the added rare earth oxides. The fracture toughness resulting from the addition of Lu_2O_3 was higher than that of Y_2O_3, whereas that of La_2O_3 was lower. The debonding angle has been measured to qualitatively evaluate the bonding strength of grain boundaries in the Si_3N_4 ceramics prepared by adding MgO and rare earth oxides.[16] It was found that the critical angle for crack debonding depends on the rare earth oxide added, and thus the grain boundary bonding of Lu_2O_3 is stronger than that of La_2O_3. This is the same tendency as the grain-boundary fracture toughness directly measured in the present study, in spite of using Al_2O_3 as a sintering aid. The fracture toughness or strength of the grain boundaries in Si_3N_4 ceramics is related to the residual stress resulting from differences in the coefficient of thermal expansion of SiAlON glass existing at the grain boundaries and that of Si_3N_4.[33] The coefficient of thermal expansion of SiAlON glass is higher than that of Si_3N_4, and the coefficient increases with increasing ionic radius of the added rare earth ion.[34] As a result, the higher residual stress that occurs at grain boundaries containing rare earth ions with large radii degrades the bonding strength of the grain boundary. This explanation implies that the grain boundary is weaker than SiAlON glass. In consideration of the fact that the measured fracture toughness of the grain boundary was higher than the fracture toughness of SiAlON glass, the fracture toughness of the grain boundaries of Si_3N_4 ceramics can be controlled not only by the coefficient of thermal expansion but also by other factors.

Becher *et al.* reported that a crack in Si_3N_4 ceramics propagates at the interface between the Si_3N_4 grain and the intergranular glassy film or inside the intergranular glassy film.[35] In this study, we directly and stably observed the crack propagation behavior of Si_3N_4 ceramics using a scanning probe microscope on a nanoscale, which is similar to the method used in our previous study.[36] Figure 6 shows the topographic images

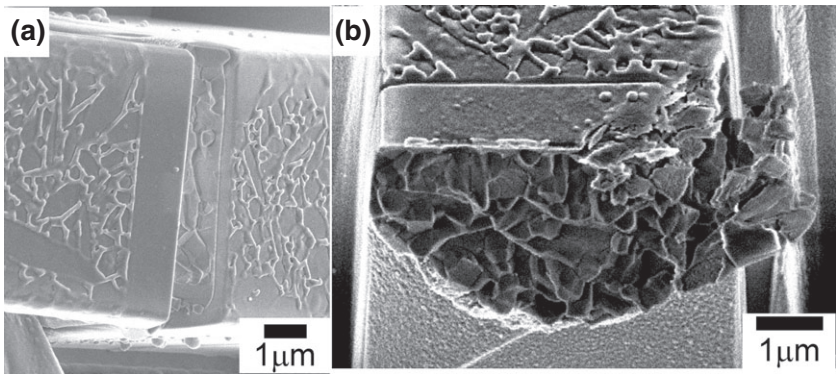

Fig. 5. Fracture surfaces of single-edge notched microcantilever beam specimens used to measure the fracture toughness of grain boundaries: (a) crack propagated along the targeted grain boundary and (b) crack that failed to propagate along the targeted grain boundary.

Table I. Fracture Toughness of Grain Boundary, Grain, and Polycrystal of Si_3N_4 Ceramics Measured Using Single-Edge Notched Microcantilever Beam Specimens

Target	Sintering aids	GPS condition	Fracture toughness	The number of the specimens
Grain boundary	Y_2O_3–Al_2O_3	1900°C-2 h	1.73 ± 0.52 $MPam^{1/2}$	5
	La_2O_3–Al_2O_3	1900°C-2 h	1.63 ± 0.60 $MPam^{1/2}$	7
	Lu_2O_3–Al_2O_3	1900°C-2 h	2.28 ± 0.37 $MPam^{1/2}$	12
Grain	Y_2O_3–Al_2O_3	1900°C-2 h	2.77 ± 0.54 $MPam^{1/2}$	8
Polycrystal	Y_2O_3–Al_2O_3	1800°C-2 h	1.92 ± 0.37 $MPam^{1/2}$	10

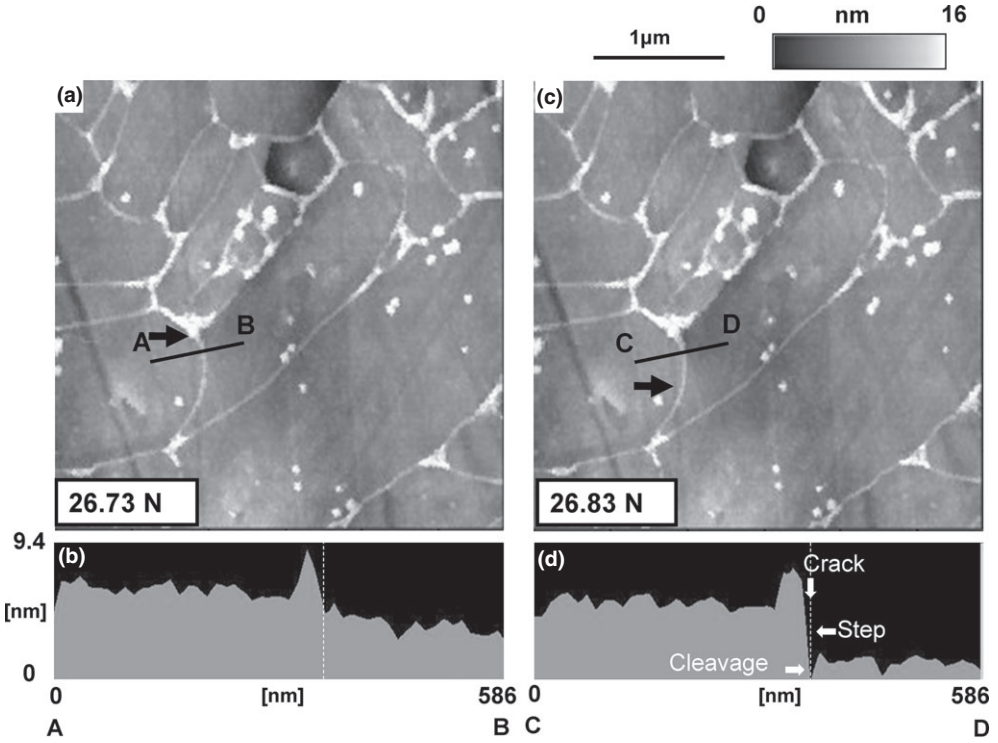

Fig. 6. Scanning probe microscopic images of *in situ* observation of crack propagation in Si_3N_4 ceramics. Arrows indicate the crack tips; (a) and (c) are topographic images before and after crack propagation, respectively, and the bottom-left numbers in (a) and (c) are applied loads to the specimens; (b) and (d) indicate the surface profiles of A–B and C–D in the topographic images, respectively.

and the cross-sectional view of the Si_3N_4 ceramics in the *in situ* observation of crack propagation. These images were taken using plasma-etched surfaces so that grain boundaries can be detected using the convex portion, which results from differences in the etching rate between the Si_3N_4 itself and the intergranular glassy film [Fig. 6(b)]. The height of the convex portion measured in this study was approximately 2 nm. Before crack propagation in the grain boundary [Fig. 6(a)], a symmetrical profile across the grain boundary was observed [Fig. 6(b)]. As increasing the applied load, a small cleavage was observed, which means that the crack propagated and opened by loading. Furthermore, after crack propagation, a small step of about 3 nm also formed on one side of the grain boundary [Figs 6(c) and (d)]. This indicates that the grain boundary fracture occurred not in the intergranular glassy film but in the interface between the glass phase and the Si_3N_4 grain. Shibata *et al.* investigated the interfacial structure in Si_3N_4 ceramics by high-angle annular dark-field scanning transmission electron microscopy (HAADF-STEM) analysis.[37,38] They found that rare-earth ions exist in the boundary between Si_3N_4 and glassy

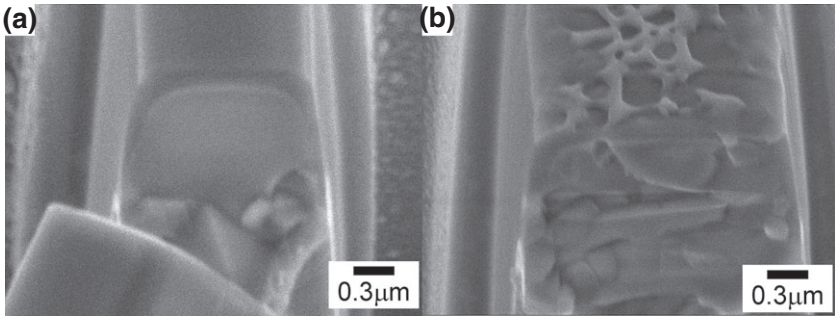

Fig. 7. Fracture surface of single-edge notched microcantilever beam specimens used to measure the fracture toughness of (a) a single Si_3N_4 grain and (b) polycrystals.

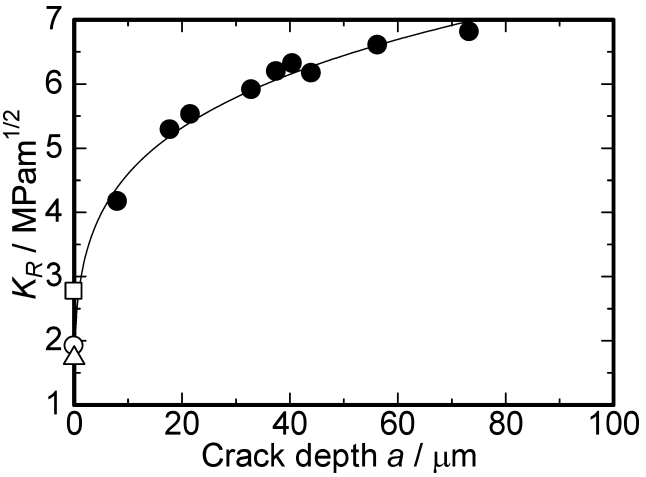

Fig. 8. R curve in short crack length of Si_3N_4 ceramics prepared by adding Y_2O_3 measured by SCF method. ●: Fracture toughness measured by SCF method, ○: Fracture toughness of polycrystal, □: Fracture toughness of grain, and △: Fracture toughness of grain boundary. A solid line is a result of regression analysis by power function ($K_R = Aa^m$).

phase and a larger amount of La^{3+} ions are located on the interface than Lu^{3+} ions, which means that the segregation of rare earth ions increases with increasing ionic radius. When the number of segregated ions increases on a Si_3N_4 grain, O (N)–Si–N bonding at the interface, which should have higher covalent bonding than rare earth ions and O or N, decreased. Although the Si_3N_4 ceramics used in this study contained Al_2O_3, which means that the grain is not exactly pure β-Si_3N_4 but rather β-SiAlON, thus having a very small of Al and O, and a glass phase that includes Al, Becher *et al.* also reported that the tendency of the segregation of rare-earth ions is the same as that of Si_3N_4 ceramics prepared by adding MgO.[39] Consequently, the highest grain-boundary fracture toughness was shown in the Si_3N_4 ceramics prepared by adding Lu_2O_3, followed by Y_2O_3 and La_2O_3 in descending order.

(2) Fracture Toughness of a Grain of Si_3N_4 Ceramics

Figure 7(a) shows the fracture surface of the single-edge notched microcantilever beam specimen used to measure the fracture toughness of a single grain after the bending test. The fracture surface was very flat, which indicates mode I fracture toughness of β-Si_3N_4.

Table I lists the fracture toughness of β-Si_3N_4 grains. The average fracture toughness of the grain was 2.77 MPa m$^{1/2}$, which is higher than that of the grain boundary. By applying *t*-test at 95% confidence, the difference between the fracture toughness of grain and grain boundary prepared by adding Lu_2O_3 was found to be statistically significant (*P*-value for two-side test was 0.0497). Hirosaki *et al.* reported that the fracture toughness of β-Si_3N_4 estimated by molecular dynamics simulations was 0.7 MPa m$^{1/2}$ and its calculated value from the surface energy and elastic constant was 0.89 MPa m$^{1/2}$.[40] The value directly measured in this study is higher than those reported in previous studies, indicating that some energy dissipation other than surface formation possibly occurred during the fracture of β-Si_3N_4. Furthermore, the current result was slightly higher than that of α-Si_3N_4,[41] which probably resulted from differences in the crystal structure and crystal stability.[42]

(3) Fracture Toughness of Polycrystals of Si_3N_4 Ceramics

The sintering aids used in the sample to measure the fracture toughness of polycrystals were Y_2O_3 and Al_2O_3. As shown in Fig. 7(b), the fracture surface was composed of several grains located at the notch tip in the single-edge notched microcantilever beam specimens. Fracture of the specimens occurred along the grain boundaries with crack deflection. The fracture toughness of a polycrystal of Si_3N_4 measured using a single-edge notched microcantilever beam specimen is also listed in Table I. The value was 1.92 MPa m$^{1/2}$, which is intermediate between the fracture toughness of the grain and that of the grain boundary. As a result of *t*-test, it was found that the difference between the fracture toughness of the grain boundary resulting from addition of Lu_2O_3 and that of the polycrystals was statistically significant (*P*-value for two-side test was 0.0029). This sequence is very reasonable in consideration of the fact that the fracture mode of the Si_3N_4 ceramics was intergranular fracture.

Figure 8 shows the *R* curve for a short crack length of the Si_3N_4 ceramics prepared by adding Y_2O_3 measured by surface cracks using the flexure method. The value of the fracture toughness measured using single-edge notched microcantilever beam specimens is also plotted in the figure. The regression curve by power low [$K_R = Aa^m$ (*a*: crack depth, *A* and *m*: constants)] is also shown in the figure. It is shown that the interpolated value of the *R* curve at a crack depth of 0 μm roughly agrees with the fracture toughness of a polycrystal measured using single-edge notched microcantilever specimens. The initial value of the *R* curve, K_{I0}, is the fracture toughness without any grain bridging or pullout. The reason for the good agreement was because of the very small size of the microcantilever beam specimens.

IV. Conclusions

The fracture toughness of grains, grain boundaries, and polycrystals of Si_3N_4 ceramics was successfully evaluated using single-edge notched microcantilever beam specimens. The fracture toughness of grain boundary depends on the rare-earth oxide added as a sintering aid. The fracture toughness of grain boundary was higher than the fracture toughness of the SiAlON glass that usually exists as the intergranular glassy film, which suggests that the intergranular glassy film structure should be different from that of the bulk SiAlON

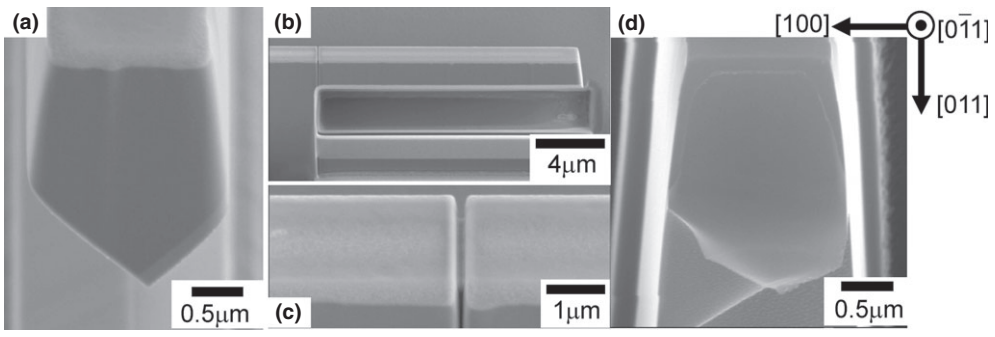

Fig. A1. (a), (b) and (c) Single-edge notched microcantilever beam specimens of single-crystal Si and (d) fracture surface of single-crystal Si.

glass. The fracture toughness of Si_3N_4 grains was higher than the value estimated from *ab initio* calculations. The fracture toughness of a polycrystal of Si_3N_4 ceramics was intermediate between those of the grain and grain boundary, and it agreed with the initial value of the *R* curve.

Appendix
Validation of the testing method

To validate the testing method, the fracture toughness of Si was measured using single-edge notched microcantilever beam specimens machined by FIB technique. Figure A1(a)–(c) shows the single-edge notched microcantilever beam specimens of single-crystal Si. The surface of the single crystal was (011) and the notch was induced along (011), which means that the fracture surface was (011) and the crack propagating direction was <011>. As shown in Fig. A1 (d), the cleavage fracture occurred on the surface of (011). The measured fracture toughness K_{IC} of single-crystal Si is 1.17 ± 0.13 MPa $m^{1/2}$, which agrees quite well with the results of a previous study.[43] It was confirmed that measuring the fracture toughness using single-edge notched microcantilever beam specimens is valid. Although we have to minimize the influence of Ga ions induced during the machining process on the experimental value, it was also confirmed that the effect is very small.

Acknowledgment

This work was partially supported by Industrial Technology Research Grant Program in 2011 from New Energy and Industrial Technology Development Organization (NEDO) of Japan, and Research Program for Strategic Seeds from Kanagawa Academy of Science and Technology (KAST) of Japan, and JSPS KAKENHI Grant Number 21686062.

References

[1]H. Kawamura and S. Yamamoto, "Improvement of Diesel Engine Startability by Ceramic Glow Plug Start System"; Society of Automotive Engineers Paper No. 830580 (1983).
[2]K. Komeya and H. Kotani, "Development of Ceramic Antifriction Bearing," *JSAE Rev.*, **7**, 72–9 (1986).
[3]Y. Zhou, H. Hyuga, D. Kusano, Y. Yoshizawa, and K. Hirao, "A Tough Silicon Nitride Ceramic with High Thermal Conductivity," *Adv. Mater.*, **23** [39] 4563–7 (2011).
[4]G. R. Terwillinger and F. F. Lange, "Pressureless Sintering of Si_3N_4," *J. Mater. Sci.*, **10** [7] 1169–74 (1975).
[5]M. Mitomo, "Pressure Sintering of Si_3N_4," *J. Mater. Sci.*, **11** [6] 1103–7 (1976).
[6]H. J. Kleebe, M. K. Cinibulk, R. M. Cannon, and M. Ruhle, "Statistical Analysis of the Intergranular Film Thickness in Silicon Nitride," *J. Am. Ceram. Soc.*, **76**, 1969–77 (1993).
[7]S. Hampshire and M. J. Pomeroy, "Oxynitride Glasses," *Int. J. App. Ceram. Tech.*, **5** [2] 155–63 (2008).
[8]S. G. Guo, N. Hirosaki, Y. Yamamoto, T. Nishimura, and M. Mitomo, "Strength Retention in Hot-Pressed Si_3N_4 Ceramics with Lu_2O_3 Additives After Oxidation Exposure in Air at 1500°C," *J. Am. Ceram. Soc.*, **85** [6] 1607–9 (2002).
[9]K. Komeya, M. Komatsu, T. Kameda, Y. Goto, and A. Tsuge, "High-Strength Silicon Nitride Ceramics Obtained by Grain-Boundary Crystallization," *J. Mater. Sci.*, **26**, 5513–6 (1991).
[10]J. Tatami, E. Kodama, H. Watanabe, H. Nakano, T. Wakihara, K. Komeya, T. Meguro, and A. Azushima, "Fabrication and Wear Properties of TiN Nanoparticle-Dispersed Si_3N_4 Ceramics," *J. Ceram. Soc. Jpn.*, **116**, 749–54 (2008).
[11]R. L. Stewart and R. C. Bradt, "Fracture of Single Crystal $MgAl_2O_4$," *J. Mater. Sci.*, **15**, 67–72 (1981).
[12]K. Hayashi, M. Ashizuka, R. C. Bradt, and H. Hirano, "Cleavage of Gallium Phosphide," *Mater. Lett.*, **1**, 116–8 (1982).
[13]S. M. Wiederhorn, "Fracture of Sapphire," *J. Am. Ceram. Soc.*, **52** [9] 485–91 (1969).
[14]J. Tatami, T. Harada, K. Yasuda, and Y. Matsuo, "Influence of Twist Angle on the Fracture Toughness of (0001) Twist Boundary of Alumina," *Ceram. Eng. Sci. Proc.*, **19** [3] 211–8 (1998).
[15]K. Yasuda, T. Harada, J. Tatami, and Y. Matsuo, "Evaluation of Fracture Toughness of (0001) Twist Boundary Using Alumina Bicrystal," *J. Ceram.Soc. Jpn.*, **106**, 372–6 (1998).
[16]S. Fünfschilling, T. Fett, M. J. Hoffmann, R. Oberacker, T. Schwind, J. Wippler, T. Böhlke, H. Özcoban, G. A. Schneider, P. F. Becher, and J. J. Kruzic, "Mechanisms of Toughening in Silicon Nitrides: The Roles of Crack Bridging and Microstructure," *Acta Mater.*, **59**, 3978–89 (2011).
[17]J. Tatami, K. Yasuda, Y. Matsuo, and S. Kimura, "Stochastic Analysis on Crack Path of Polycrystalline Ceramics Based on the Difference Between the Released Energies in Crack Propagation," *J. Mater. Sci.*, **32** [9] 2341–6 (1997).
[18]R. Terao, J. Tatami, T. Meguro, and K. Komeya, "Fracture Behavior of AlN Ceramics with Rare Earth Oxides," *J. Eur. Ceram. Soc.*, **22** [7] 1051–9 (2002).
[19]T. Ohji, K. Hirao, and S. Kanzaki, "Fracture Resistance Behavior of Highly Anisotropic Silicon Nitride," *J. Am. Ceram. Soc.*, **78**, 3125–8 (1995).
[20]P. F. Becher, E. Y. Sun, K. P. Plucknett, K. B. Alexander, C. H. Hsueh, H. T. Lin, S. B. Waters, C. G. Westmoreland, E. S. Kang, K. Hirao, and M. E. Brito, "Microstructural Design of Silicon Nitride with Improved Fracture Toughness: I, Effects of Grain Shape and Size," *J. Am. Ceram. Soc.*, **81** [11] 2821–30 (1998).
[21]R. B. Greene, S. Fünfschilling, T. Fett, M. J. Hoffmann, and J. J. Kruzic, "Fatigue Crack Growth Behavior of Silicon Nitride: Roles of Grain Aspect Ratio and Intergranular Film Composition," *J. Am. Ceram. Soc.*, **96** [1] 259–65 (2013).
[22]J. Tatami, I. W. Chen, Y. Yamamoto, M. Komatsu, K. Komeya, D. K. Kim, T. Wakihara, and T. Meguro, "Fracture Resistance and Contact Damage of TiN Particle Reinforced Si_3N_4 Ceramics," *J. Ceram. Soc. Jpn.*, **114**, 1049–53 (2006).
[23]S. Fünfschilling, T. Fett, R. Oberacker, M. J. Hoffmann, G. A. Schneider, P. F. Becher, and J. J. Kruzic, "Crack-Tip Toughness from Vickers Crack-Tip Opening Displacements for Materials with Strongly Rising R-Curves," *J. Am. Ceram. Soc.*, **94** [6] 1884–92 (2011).
[24]T. Fett, S. Fünfschilling, M. J. Hoffmann, R. Oberacker, H. Jelitto, and G. A. Schneider, "R-Curve Determination for the Initial Stage of Crack Extension in Si_3N_4," *J. Am. Ceram. Soc.*, **91** [11] 3638–42 (2008).
[25]T. Fett, D. Creek, S. Wagner, G. Rizzi, and C. A. Volkert, "Fracture Toughness Test with a Sharp Notch Introduced by Focussed Ion Beam," *Int. J. Fracture*, **153**, 85–92 (2008).
[26]S. Bechtle, H. Özcoban, E. D. Yilmaz, T. Fett, G. Rizzi, E. T. Lilleodden, N. Huber, A. Schreyer, M. V. Swain, and G. A. Schneider, "A Method to Determine Site-Specific, Anisotropic Fracture Toughness in Biological Materials," *Scripta Mater.*, **66**, 515–8 (2012).
[27]S. Fuenfschilling, T. Fett, M. J. Hoffmann, R. Oberacker, H. Oezcoban, G. A. Schneider, P. Brenner, D. Gerthsen, and R. Danzer, "Estimation of the High-Temperature R-Curve for Ceramics from Strength Measurements Including Specimens with Focused Ion Beam Notches," *J. Am. Ceram. Soc.*, **93**, 2411–4 (2010).
[28]G. R. Irwin, "Analysis of Stresses and Strains Near the End of a Crack Traversing a Plate," *Trans. ASME, J. Appl., Mech.*, **24**, 361–4 (1957).
[29]K. Yasuda, T. Taguchi, J. Tatami, and Y. Matsuo, "Estimation of Short Crack R-Curves of Polycrystalline Ceramics by the Surface Crack in Flexure Method," *Ceram. Trans.*, **133**, 115–20 (2002).
[30]J. C. Newman Jr. and I. S. Raju, "An Empirical Stress-Intensity Factor Equation for the Surface Crack," *Eng. Fract. Mech.*, **15** [1–2] 185–92 (1981).
[31]R. E. Loehman, "Preparation and Properties of Yttrium-Silicon-Aluminum Oxynitride Glasses," *J. Am. Ceram. Soc.*, **62**, 491–4 (1979).
[32]A. Bhatnagar, M. J. Hoffmann, and R. H. Dauskardt, "Fracture and Subcritical Crack-Growth Behavior of Y-Si-Al-O-N Glasses and Si_3N_4 Ceramics," *J. Am. Ceram. Soc.*, **83**, 585–96 (2000).
[33]E. Y. Sun, P. F. Becher, K. P. Plucknett, C. H. Hsueh, K. B. Alexander, S. B. Waters, C. G. Westmoreland, K. Hirao, and M. E. Brito, "Microstructural Design of Silicon Nitride with Improved Fracture Toughness: II, Effects of Yttria and Alumina Additives," *J. Am. Ceram. Soc.*, **81**, 2831–40 (1998).
[34]F. Lofaj, R. Statet, M. J. Hoffmann, and A. R. de Arellano López, "Thermal Expansion and Glass Transition Temperature of the Rare-Earth Doped Oxynitride Glasses," *J. Eur. Ceram. Soc.*, **24**, 3377–85 (2004).
[35]P. F. Becher, G. S. Painter, M. J. Lance, S. Ii, and Y. Ikuhara, "Direct Observations of Debonding of Reinforcing Grains in Silicon Nitride Ceramics Sintered with Yttria Plus Alumina Additives," *J. Am. Ceram. Soc.*, **88** [122] 2–1226 (2005).
[36]K. Yasuda, J. Tatami, Y. Matsuo, and S. Kimura, "In-Situ Observation of Ceramics Using Scanning Electron Microscope," *J. Mater. Sci. Jpn.*, **33**, 238–44 (1997).
[37]N. Shibata, G. S. Painter, R. L. Satet, M. J. Hoffmann, S. J. Pennycook, and P. F. Becher, "Rare-Earth Adsorption at Intergranular Interfaces in Silicon Nitride Ceramics: Subnanometer Observations and Theory," *Phys. Rev. B*, **72**, 140101(R) (2005).
[38]P. F. Becher, G. S. Painter, N. Shibata, R. L. Satet, M. J. Hoffmann, and S. J. Pennycook, "Influence of Additives on Anisotropic Grain Growth in Silicon Nitride Ceramics," *Mater. Sci. Eng., A*, **422**, 85–91 (2006).
[39]P. F. Becher, N. Shibata, G. S. Painter, F. Averill, K. van Benthem, H. T. Lin, and S. B. Waters, "Observation on the Influence of Secondary Me Oxide Additives (Me=Si, Al, Mg) on the Microstructural Evolution and Mechanical Behavior of Silicon Nitride Ceramics Containing RE_2O_3," *J. Am. Ceram. Soc.*, **93** [2] 570–80 (2010).
[40]N. Hirosaki, S. Ogata, and H. Kitagawa, "Molecular Dynamics Study of the Stress Distribution Near a Crack Tip in Beta-Silicon Nitride," *Mater. Sci. Res. Inter.*, **5–4**, 253–7 (1999).
[41]I. E. Reimanis, H. Suematsu, J. J. Petrovic, and T. E. Mitchel, "Mechanical Properties of Single Crystal α-Si_3N_4," *J. Am. Ceram. Soc.*, **79**, 2065–73 (1996).
[42]R. Grun, "The Crystal Structure of β-Si_3N_4; Structural and Stability Considerations Between α- and β-Si_3N_4," *Acta Cryst.*, **35**, 800–4 (1979).
[43]T. Ando, X. Li, S. Nakao, T. Kasai, H. Tanaka, M. Shikida, and K. Sato, "Fracture Toughness Measurement of Thin Film Silicon," *Fatigue Fract. Eng. Mater. Struct.*, **28**, 687–94 (2005). □